transfer then occurs to produce the reaction products. In this way we account for the almost 50% overall volume change in terms of $\Delta V^{\ddagger}$. An important aspect of our suggestion is that the large positive $\Delta V^{\ddagger}$ mainly results from volume changes associated with the iron center in agreement with arguments presented before.[14,25,27]

We now turn to a discussion of the light-induced electron-transfer reaction. The significant increase in k_2 with increasing light intensity found in this study is in good agreement with similar findings reported before.[13,15] The bridged complexes exhibit MLCT bands around 625 nm such that irradiation at this wavelength (usually selected to monitor the thermal redox reaction) results in a photoinduced electron-transfer process. The quantum yield for the latter process was reported[15] to be 0.9 ± 0.15 for $Co(NH_3)_4(pzc)^{2+}$ and $Co(NH_3)_5(pz)^{3+}$ and 0.020 for $Co(en)_2(pzc)^{2+}$, which accounts for the fact that no significant effect of light intensity was observed in the latter case. A very significant finding of this study is that, under the conditions where a significant acceleration by light occurs, the observed pressure dependence almost completely disappears. For the $Co(NH_3)_4(pzc)^{2+}$ complex the rate constant increases by almost a factor 4 such that the thermal reaction makes only a small contribution at high light intensities. In the case of the $Co(NH_3)_5pz^{3+}$ complex, some contribution from the thermal reaction is still possible at high light intensities, and in fact a correction for this contribution results in an almost zero volume of activation for the photoinduced process.

The pressure independence of the photoinduced electron-transfer process can be interpreted in the following way. During MLCT excitation electron density is transferred from Fe(II) to the pyrazine or pyrazinecarboxylate ligand as shown in (7).[15] The

$$(NC)_5Fe^{II}(\mu\text{-}L)Co^{III}(NH_3)_5 \xrightarrow{h\nu} (NC)_5Fe^{III}(\mu\text{-}L^-)Co^{III}(NH_3)_5 \quad (7)$$

subsequent first-order process observed during irradiation must involve the transfer of the electron from the bridging ligand to the cobalt center. According to the pressure independence of this process, no significant volume change is associated with this reaction, which means that the major volume increase occurs during the oxidation of Fe(II). Our observation that the subsequent reduction of Co(III) following MLCT excitation does not lead to a significant volume increase directly supports our earlier arguments (see above) presented to account for the $\Delta V^{\ddagger}$ data associated with the thermally induced electron-transfer reaction.[14,25-27] In general, this finding does contradict earlier arguments in favor of the suggestion that the major volume change that occurs in related electron-transfer reactions is associated with volume changes on the cobalt center.[13,28] It must be kept in mind that the quantum yield for these photoinduced reactions is almost unity. This means that other deactivation routes then the photochemical reaction (i.e. radiationless and radiative deactivation) play no significant role. This would require that the lifetime of the MLCT excited state must be long so that electron transfer from the coordinated N atom to the Co(III) center can occur. Since the quantum yield is close to unity, any effect of pressure on the photochemical rate constant will not affect the quantum yield. This means that $Fe^{III}(\mu\text{-}L^-)Co^{III}$ is produced rapidly during the continuous irradiation and undergoes L-to-Co(III) electron transfer during the first-order decay.

We believe that the results of this investigation support the operation of a two-step electron-transfer mechanism for the photoinduced intramolecular redox process, i.e. the chemical mechanism.[29]

Acknowledgment. We gratefully acknowledge financial support from the Deutsche Forschungsgemeinschaft, Fonds der Chemischen Industrie, and Volkswagen-Stiftung. A stipend from the Junta de Andalucia, which enabled P.G. to participate in this study, is greatly appreciated. Stimulating discussions with Dr. J. Burgess (University of Leicester, Leicester, U.K.) on the investigated reactions are kindly acknowledged.

Registry No. $Fe(CN)_5H_2O^{3-}$, 18497-51-3; $Co(NH_3)_4pzc^{2+}$, 61546-76-7; $Co(en)_2pzc^{2+}$, 56238-31-4; $(NH_3)_4Co^{III}(\mu\text{-pzc})Fe^{II}(CN)_5$, 61546-71-2; $(en)_2Co^{III}(\mu\text{-pzc})Fe^{II}(CN)_5$, 56238-33-6; $(NH_3)_5Co^{III}(\mu\text{-pz})Fe^{II}(CN)_5$, 66840-84-4.

(28) Kanesato, M.; Ebihara, M.; Sasaki, Y.; Saito, K. *J. Am. Chem. Soc.* **1983**, *105*, 5711.
(29) Gould, E. S. *Acc. Chem. Res.* **1985**, *18*, 22.

Contribution from the Department of Chemistry and the Center for Organometallic Research, University of North Texas, Denton, Texas 76203-5068, and Institute for Inorganic Chemistry, University of Witten/Herdecke, Stockumer Strasse 10, 5810 Witten, FRG

Octahedral Metal Carbonyls. 71.[1] Kinetics and Mechanism of Benzene Displacement from Photogenerated [(η^2-Benzene)$Cr(CO)_5$]

Shulin Zhang,[2] Gerard R. Dobson,*[,2] Volker Zang,[3] Hari C. Bajaj,[3] and Rudi van Eldik*[,3]

Received December 7, 1989

Pulsed laser flash photolysis of $Cr(CO)_6$ in $Cr(CO)_6$/benzene/L solutions (L = piperidine, 1-hexene, pyridine) affords as the predominant reaction species [(η^2-benzene)$Cr(CO)_5$] (**1**) in which benzene is coordinated to Cr via an "isolated" C=C bond. **1** reacts with L on the microsecond time scale to afford $LCr(CO)_5$ products. On the basis of kinetics studies over a wide range of benzene and L concentrations ([benzene] = 2.8-10.1 M; [L] = 1.2-6.5 M), a temperature range of 5-35 °C, pressures to 100 MPa, and isotopic labeling studies (benzene-d_6), it is concluded for L = 1-hexene and piperidine that the displacement of benzene from **1** takes place by means of reversible formation of the $[Cr(CO)_5]$ intermediate via a transition state in which benzene is bonded to Cr, forming a "σ-complex", or via an agostic C-H-Cr interaction. For L = pyridine at very high [py], an interchange process involving displacement of benzene also may be accessible. The observed rate laws incorporate the concentrations of all chemical species present in solution in significant concentration after flash photolysis. Thus benzene/L solutions may be classified as "reactive solutions" in the presence of $[Cr(CO)_5]$. The upper limit of the benzene-Cr bond strength is estimated from activation data to be 9.4 (1) kcal/mol.

Introduction

Coordinatively unsaturated transition-metal complexes are of increasing interest because they often are implicated as active species in homogeneous catalysis. In this regard it has been noted that "a site of coordinative unsaturation is perhaps the single important property of a homogeneous catalyst".[4] However, it is now widely recognized that in many cases the species produced in predominant concentration after metal-ligand bond fission are

(1) Part 70: Zhang, S.; Dobson, G. R. *Inorg. Chim. Acta* **1989**, *165*, 11.
(2) University of North Texas.
(3) University of Witten/Herdecke.
(4) Collman, J. P. *Acc. Chem. Res.* **1968**, *1*, 136.

0020-1669/90/1329-3477$02.50/0

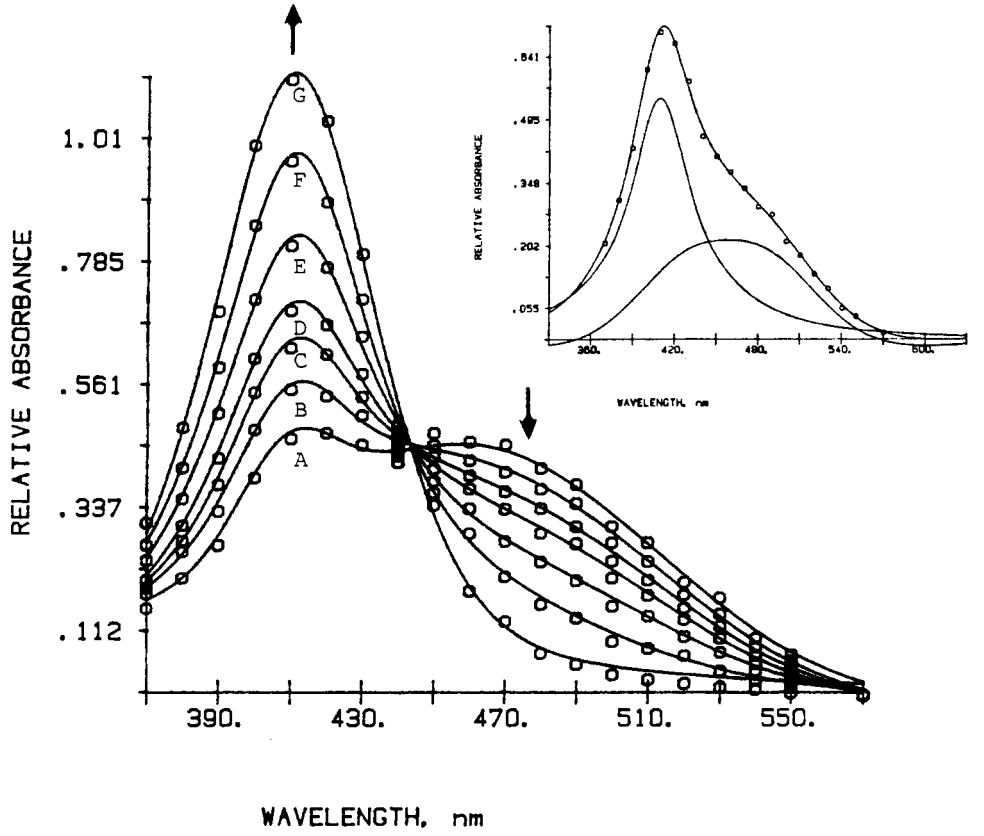

Figure 1. Time-resolved spectra obtained after flash photolysis of $Cr(CO)_6$ in piperidine (2.531 M)/benzene (8.344 M) solution at 25.0 °C. Time after the flash: (A) 0.5 μs; (B) 2.0 μs; (C) 3.5 μs; (D) 5.0 μs; (E) 8.5 μs; (F) 16 μs; (G) 67 μs. Inset: Plot of relative absorbance vs wavelength for spectrum E showing resolution of plot into spectra for [(η^2-benzene)$Cr(CO)_5$] (λ_{max} = 458 (10) nm) and (pip)$Cr(CO)_5$ (λ_{max} = 410 (1) nm).

not coordinatively unsaturated but are specifically solvated.

$Cr(CO)_6$ has served as an exemplar for studies of solvation in coordinatively unsaturated intermediates. It has been found that upon Cr–CO bond fission in $Cr(CO)_6$, the $[Cr(CO)_5]$ produced reacts very rapidly with solvent to afford [(solvent)$Cr(CO)_5$] species,[5] in which the solvent molecule occupies a position in the inner coordination sphere of $[Cr(CO)_5]$ and forms a coordinate covalent bond with the metal atom. The solvation process has been widely studied, but mechanisms of solvent displacement have been investigated in less detail.[6-8] Yet the mechanism of desolvation has crucial bearing on catalytic selectivity. Where the solvent is an alkane or arene, there has been much interest in the nature of the solvent–metal interaction, since this interaction is the first step along the reaction coordinate to C–H bond activation by transition metals.[9] $Cr(CO)_6$ has also been implicated as the precursor to photochemically generated catalysts involved in olefin isomerization, hydrogenation, and hydrosilylation reactions.[10] Thus there are compelling reasons to study the mechanisms of desolvation of [(solvent)$Cr(CO)_5$] intermediates, particularly in hydrocarbon solution. Herein are reported kinetics studies of the displacement of benzene (bz) from photogenerated [(bz)$Cr(CO)_5$] by Lewis bases, L = 1-hexene, piperidine, and pyridine (hex, pip, and py, respectively), to afford $LCr(CO)_5$ products. Since bz forms a coordinate covalent bond to chromium in photogenerated [(bz)$Cr(CO)_5$], it can be regarded as a "reactive solvent" rather than a dispersive medium; it has been so considered in this work. Thus rate studies for solutions in which pip, py, and hex as well as bz are present in predominant concentration have been carried out.

Experimental Section

Materials. $Cr(CO)_6$ (Pressure Chemical Co.) was vacuum-sublimed before use. Piperidine (Aldrich) and py (Fisher Scientific) were distilled over KOH under nitrogen immediately before use. 1-Hexene (Aldrich) was distilled over anhydrous $MgSO_4$. Benzene (Mallinckrodt Analyzed reagent) was fractionally distilled from sodium under nitrogen, while bz-d_6 (Norell, Inc., 99.5% D) was used without further purification.

Laser Flash Photolysis Studies. The pulsed laser flash photolysis apparatus used for the ambient-pressure studies (at the University of North Texas) employed a Lumonics TE-430 excimer laser (XeF; 351 nm; 14 ns fwhi), the beam from which was focused on the observation cell; other details with regard to the equipment employed have been given elsewhere.[11] Flash photolysis studies at variable high pressure were carried out at the Center for Fast Kinetics Research (CFKR), University of Texas at Austin. The pulsed laser flash photolysis apparatus utilized at CFKR[12] and the variable-pressure equipment[13] also have been described previously. In these studies the temperature was controlled by employing a Haake D8 circulator and monitored by using a Keithley 872 digital thermometer. In typical reactions carried out at either ambient or high pressure, a solution ca. 3.5×10^{-3} M in $Cr(CO)_6$, also containing large excesses of L and bz (to insure pseudo-first-order reaction conditions), were employed. Both bz and L were weighed so that their concentrations would be known with accuracy. No significant differences in traces of ln (absorbance) vs time taken after a single flash or after multiple flashes were observed. The pseudo-first-order rate constants, k_{obsd}, were obtained as averages of 1–10 traces and are presented in Appendix A (supplementary material). The kinetics data were analyzed

(5) (a) Welch, J. A.; Peters, K. S.; Vaida, V. *J. Phys. Chem.* **1982**, *86*, 1941. (b) Simon, J. D.; Peters, K. S. *Chem. Phys. Lett.* **1983**, *98*, 53. (c) Simon, J. D.; Xie, X. *J. Phys. Chem.* **1986**, *90*, 6751. (d) Simon, J. D.; Xie, X. *J. Phys. Chem.* **1987**, *91*, 5538. (e) Wang, L.; Zhu, X.; Spears, K. G. *J. Am. Chem. Soc.* **1988**, *110*, 8695. (f) Wang, L.; Zhu, X.; Spears, K. G. *J. Phys. Chem.* **1989**, *93*, 2. (g) Simon, J. D.; Xie, X. *J. Phys. Chem.* **1989**, *93*, 291. (h) Joly, A. G.; Nelson, K. A. *J. Phys. Chem.* **1989**, *93*, 2876.

(6) Asali, K. J.; Basson, S. S.; Tucker, J. S.; Hester, B. C.; Cortes, J. E.; Awad, H. H.; Dobson, G. R. *J. Am. Chem. Soc.* **1987**, *109*, 5385.

(7) Dobson, G. R.; Zhang, S. *J. Coord. Chem.* **1990**, *21*, 155.

(8) Yang, G. K.; Vaida, V.; Peters, K. S. *Polyhedron* **1988**, *7*, 1619.

(9) For reviews, see: (a) Parshall, G. W. *Acc. Chem. Res.* **1975**, *8*, 113. (b) Crabtree, R. H. *Chem. Rev.* **1985**, *85*, 245.

(10) For a review, see: Moggi, L.; Juris, A.; Sandrini, D.; Manfrin, M. F. *Rev. Chem. Intermed.* **1981**, *4*, 171.

(11) Zhang, S.; Dobson, G. R. *Inorg. Chem.* **1989**, *28*, 324.

(12) Dobson, G. R.; Dobson, C. B.; Mansour, S. E. *Inorg. Chem.* **1985**, *24*, 2179.

(13) Spitzer, M.; Gartig, F.; van Eldik, R. *Rev. Sci. Instrum.* **1988**, *59*, 2092.

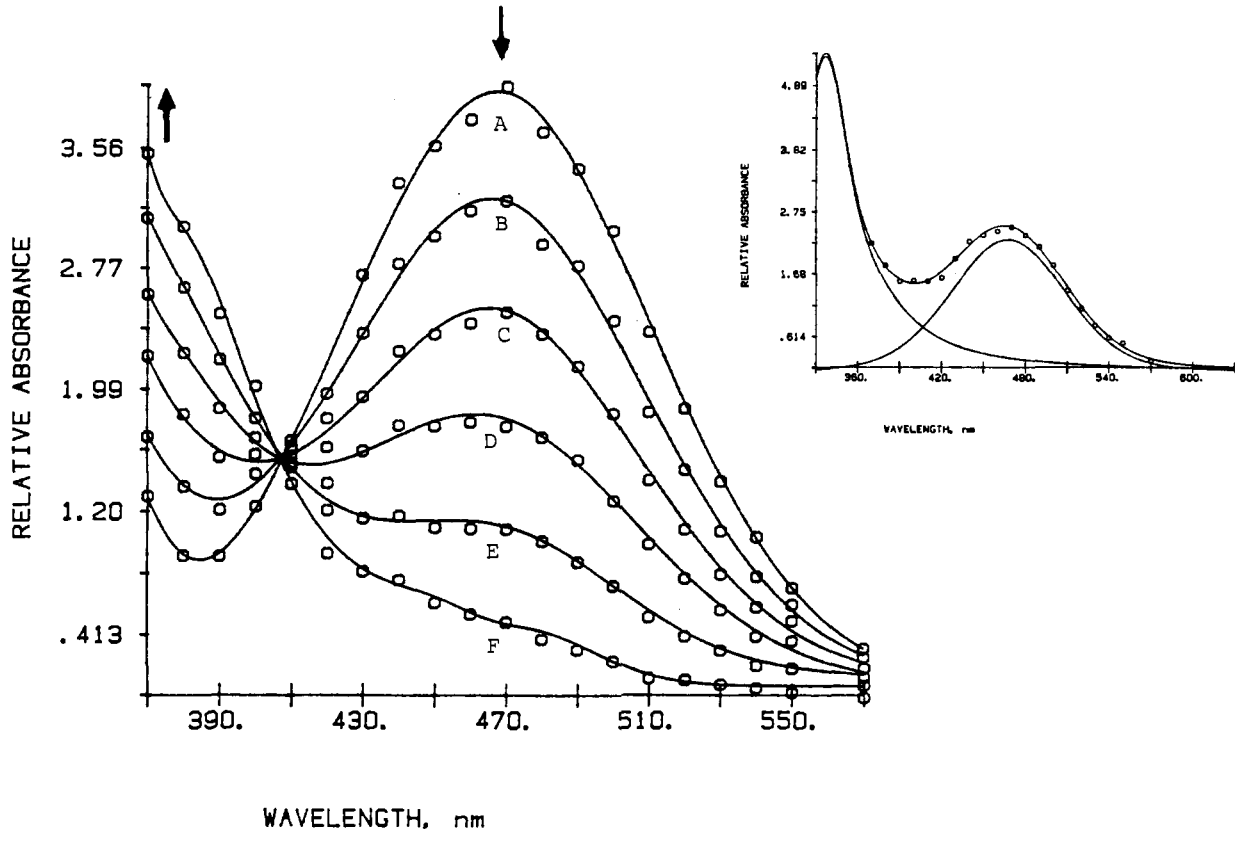

Figure 2. Time-resolved spectra obtained after flash photolysis of $Cr(CO)_6$ in 1-hexene (2.366 M)/benzene (7.832 M) solution at 25.0 °C. Time after the flash: (A) 1.0 μs; (B) 10.0 μs; (C) 22.0 μs; (D) 37.0 μs; (E) 64.5 μs; (F) 84.5 μs; (G) 134.5 μs. Inset: Plot of relative absorbance vs wavelength for spectrum E showing resolution of plot into spectra for [(η^2-benzene)$Cr(CO)_5$] (λ_{max} = 468 (2) nm) and (pip)$Cr(CO)_5$ (λ_{max} = 344 (6) nm).

by employing ASYST-based computer programs developed in-house or programs written at CFKR. Limits of error, given in parentheses as the uncertainties of the last digit(s) of the cited value, are one standard deviation.

Results and Discussion

Identification of Reaction Intermediates and Products. Figure 1 shows time-resolved spectra taken after flash photolysis of a $Cr(CO)_6$/pip/bz solution ([pip] = 2.531 M). The inset shows the resolution of one of these traces, recorded 5 μs after the flash, into spectra for the species generated initially (λ_{max} = 458 (10) nm) and at longer reaction times (λ_{max} = 410 (1) nm). The first maximum is attributable to formation of [(bz)$Cr(CO)_5$] (**1**), which has been observed in solution at 460[14] and 465[15] nm after flash photolysis. The band observed at longer reaction times has likewise been attributed to (pip)$Cr(CO)_5$.[7] Figure 2 shows analogous spectra obtained after flash photolysis of a $Cr(CO)_6$/hex/bz ([hex] = 2.366 M) solution. Resolution (inset) affords λ_{max} for **1** at 468 (2) nm and, by extrapolation,[16] λ_{max} for (η^2-hex)$Cr(CO)_5$ at 344 (6) nm. It is noted in Figures 1 and 2 that the time-resolved spectra exhibit isosbestic points, indicating conversion of **1** to single products. Thus eq 1 describes the chemical processes taking place.

$$Cr(CO)_6 \xrightarrow[bz]{h\nu} [(bz)Cr(CO)_5] \xrightarrow{k[L]} LCr(CO)_5 \qquad (1)$$

Kinetics Studies at Ambient Pressure. Since bz is a "reactive" rather than a dispersive solvent and since maximum mechanistic information can be obtained where the concentrations of bz and L are varied as widely as possible, rate data were taken over the following concentration ranges: 10.0 M > [bz] >2.8 M; 4.9 M > [pip] > 1.7 M; 5.9 M > [hex] > 1.2 M; 6.2 M > [py] > 1.2 M. Figure 3 shows typical plots of A_t vs time and of ln ($A_t - A_\infty$) vs time (A_t and A_∞ are absorbances at time t and at infinite time, respectively) for the reaction taking place after flash photolysis of a $Cr(CO)_6$/pip (2.085 M)/bz solution, monitored at 490 nm. These plots indicate that the disappearance of the photogenerated transient, **1**, obeys pseudo-first-order kinetics. Plots of the pseudo-first-order rate constants, k_{obsd}, vs [pip]/[bz] and vs [hex]/[bz] from data taken at 25 °C are illustrated in Figure 4. The observed curvature of these plots is suggestive of a mechanism involving consecutive steps, one or more of which are reversible. Thus, the most plausible mechanism involves reversible dissociation of bz from **1** followed by nucleophilic attack of L at coordinatively unsaturated [$Cr(CO)_5$] **2** (eq 2). Assuming a steady-steady

$$\underset{\mathbf{1}}{[(bz)Cr(CO)_5]} \underset{k_{-1}[bz]}{\overset{k_1}{\rightleftharpoons}} \underset{\mathbf{2}}{[Cr(CO)_5]} \xrightarrow{k_2[L]} LCr(CO)_5 \qquad (2)$$

concentration of **2**, the rate law corresponding to this mechanism is

$$-d[\mathbf{1}]/dt = k_1k_2[\mathbf{1}][L]/(k_{-1}[bz] + k_2[L]) \qquad (3)$$

In terms of the pseudo-first-order rate constant, k_{obsd}, this expression can be arranged to

$$1/k_{obsd} = 1/k_1 + (k_{-1}/k_1k_2)[bz]/[L] \qquad (4)$$

Figure 5 illustrates plots of $1/k_{obsd}$ vs [bz]/[L], which are consistent with eq 4 both in their linearity and in the coincidence of the intercepts for L = pip and hex.

For L = py, a plot of $1/k_{obsd}$ vs [bz]/[py] exhibits slight nonlinearity, with an intercept differing from those observed for L = pip and hex. However, subtraction of an amount (k_3[py]; $k_3 = 6.3 \times 10^4$ M^{-1} s^{-1} at 25.0 °C) from k_{obsd} so that the three intercepts are coincident affords a linear plot of $1/(k_{obsd} - k_3[py])$ vs [bz]/[py]. These results suggest, for L = py, the accessibility of a competing associative mechanism for benzene displacement from **1**, as shown in (5). The rate law derived from this mechanism (eq 6) is consistent with the observed kinetics. Values of

(14) Oishi, S. *Organometallics* **1988**, *7*, 1237.
(15) Kalyanasundaram, K. *J. Phys. Chem.* **1988**, *92*, 2219.
(16) This value was obtained from the best Gaussian/Lorentzian fit of the experimental data.

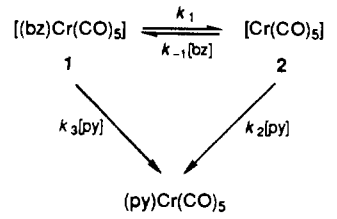

(5)

$$1/(k_{obsd} - k_3[py]) = 1/k_1 + (k_{-1}/k_1k_2)[bz]/[py] \quad (6)$$

the rate constants for displacement of bz from **1** by all three L at four temperatures are presented in Table I.

The relative rates of attack by various L at $[Cr(CO)_5]$ can be determined from values of k_2/k_{-1} obtained as intercept/slope of the reciprocal plots. These relative rates at 25 °C vary in the order py (2.72 (14)) > pip (1.93 (9)) > bz (1) > hex (0.35 (4)) and would appear to be unrelated to the strengths of the bonds being formed, which vary in the order pip[17] ≃ py[17] > hex > bz.

It is noteworthy that the kinetics data for L = pip and hex obey the rate law shown in eq 2 over the entire concentration range, from solutions in which bz is present in predominant concentration to ones in which L predominates. This evidently is the case because interactions of bz and L at the vacant coordination site in **2** are strong when compared to other possible solvent/complex interactions.

Activation parameters for the reaction shown in eq 3 are also given in Table I. The enthalpy of activation for dissociation of bz from **1**, 9.4 (1) kcal mol, should approach the upper limit for the bond dissociation energy. The entropy of activation for bz dissociation from **1**, −2.4 (3) cal/(deg mol), also is consistent with significant residual Cr–benzene bonding in the transition state, leading to bond dissociation. It is not too different from those observed for related solvent-displacement reactions taking place via dissociative pathways[6,7] or for displacement of CO from $Cr(CO)_6$ by pip.[17]

Reactions of [(benzene)Cr(CO)$_5$] with L under Pressures to 100 MPa. The volume of activation for a ligand-exchange reaction, representing as it does the difference in the volume of the transition state and ground state, is also a useful mechanistic indicator.[18] The volume of activation is related to the rate constant and pressure according to

$$-RT(\partial \ln k/\partial P)_T = \Delta V^{\ddagger} \quad (7)$$

and, where $\Delta V^{\ddagger}$ is independent of P

$$\ln k = \text{const} - (\Delta V^{\ddagger}/RT)P \quad (8)$$

On the basis of the rate law observed for reaction of **1** with pip and hex (eq 3) and discussed as above, k_1k_2/k_{-1} was determined as a function of pressure (to 80 MPa)[19] from the slope of a plot k_{obsd} vs [L] at low [L], where $k_{-1}[bz] >> k_2[L]$ (Figure 6a). This plot, for L = pip, 0.401 M, affords a $\Delta V_{obsd}^{\ddagger}$ ($= \Delta V_1^{\ddagger} + \Delta V_2^{\ddagger} - \Delta V_{-1}^{\ddagger}$) of 4.2 (3) cm^3/mol. This value can further be resolved into $\Delta V_1^{\ddagger}$ and $\Delta V_2^{\ddagger} - \Delta V_{-1}^{\ddagger}$ through variable-pressure studies of $Cr(CO)_6$/bz/pip solutions in which [bz] and [pip] also are varied widely and in which, therefore, plots of k_{obsd} vs [pip]/[bz] (eq 3) exhibit appreciable curvature. From the corresponding plots of $1/k_{obsd}$ vs [bz]/[L] (eq 4), values of k_1 and k_2/k_{-1} at various pressures (to 100 MPa) were obtained. Data from these plots were used to obtain plots of ln k_1 vs P and ln (k_2/k_{-1}) vs P. From the first of these plots (Figure 6b) $\Delta V_1^{\ddagger}$ was determined to be +12.3 (14) cm^3/mol, a value consistent with bz–Cr bond fission. The latter plot (Figure 6c) affords $\Delta V_2^{\ddagger} - \Delta V_{-1}^{\ddagger} = -8.3$ (19) cm^3/mol, which indicates less volume collapse upon bz–Cr bond making than upon pip–Cr bond formation. While the plots in Figure 6 appear slightly curved, this curvature does not arise from the influence of the compressibility of the solvent, which is predicted to be in the opposite direction and to be small compared with the observed experimental uncertainties.[20] The close agreement between the values of $\Delta V_1^{\ddagger} + \Delta V_2^{\ddagger} - \Delta V_{-1}^{\ddagger}$ from data obtained at low [pip] and from widely varying [pip]/[bz] ratios, 4.2 (3) cm^3/mol vs 4.0 (5) cm^3/mol, supports this conclusion.

Table I. Rate Constants for Thermal Reactions Taking Place after Flash Photolysis of $Cr(CO)_6$ in Benzene and Benzene-d_6 in the Presence of Various Ligands (L) at Various Temperatures

L	solvent	T, °C	$10^{-5}k_1$, s^{-1}	k_2/k_{-1}
pip	C_6H_6[a]	5.0	0.773 (6)	2.17 (3)
		15.0	1.41 (5)	2.16 (11)
		25.0	2.57 (8)	1.93 (9)
		35.0	4.4 (2)	1.92 (14)
	C_6D_6[b]	5.0	0.98 (4)	1.47 (8)
		15.0	1.75 (4)	1.39 (4)
		25.0	3.17 (11)	1.28 (6)
		35.0	4.9 (3)	1.41 (12)
hex	C_6H_6[c]	5.0	0.76 (5)	0.26 (2)
		15.0	1.5 (2)	0.30 (4)
		25.0	2.7 (2)	0.35 (4)
		35.0	4.4 (2)	0.45 (3)
py[d]	C_6H_6	25.0	2.7 (1)	2.72 (14)

[a] $\Delta H_1^{\ddagger} = 9.4$ (1) kcal/mol, $\Delta S_1^{\ddagger} = -2.4$ (3) cal/(deg mol), $\Delta H_2^{\ddagger} - \Delta H_{-1}^{\ddagger} = -0.8$ (3) kcal/mol, $\Delta S_2^{\ddagger} - \Delta S_{-1}^{\ddagger} = -1.4$ (10) cal/(deg mol). [b] $\Delta H_1^{\ddagger} = 8.6$ (3) kcal/mol, $\Delta S_1^{\ddagger} = -4.5$ (10) cal/(deg mol), $\Delta H_2^{\ddagger} - \Delta H_{-1}^{\ddagger} = -0.3$ (5) kcal/mol, $\Delta S_2^{\ddagger} - \Delta S_{-1}^{\ddagger} = -0.6$ (24) cal/(deg mol). [c] $\Delta H_1^{\ddagger} = 9.4$ (4) kcal/mol, $\Delta S_1^{\ddagger} = -2.2$ (12) cal/(deg mol), $\Delta H_2^{\ddagger} - \Delta H_{-1}^{\ddagger} = +3.0$ (4) kcal/mol, $\Delta S_2^{\ddagger} - \Delta S_{-1}^{\ddagger} = +8.8$ (15) cal/(deg mol). [d] Calculated after subtraction of k_s[py]; see the text.

Reaction of [(benzene-d_6)Cr(CO)$_5$] with pip. Several possible bonding sites to Cr exist for the benzene molecule. Stolz, Haas, and Sheline suggested, on the basis of carbonyl stretching data, that bonding in $[(bz)W(CO)_5]$ involves the whole aromatic ring.[21] However, more recent NMR[22] and X-ray[23] studies have supported "edge-on" coordination of aromatic rings to transition-metal atoms via "isolated" double bonds. A third mode of bonding of aromatic and aliphatic hydrocarbons to a transition metal is via a three-center, two-electron C–H–M "agostic" interaction.[24] A theoretical treatment by Saillard and Hoffmann has supported "end-on" agostic bonding in $(CH_4)Cr(CO)_5$;[25] a "σ-complex" in which the C–H σ-bond interacts with the transition metal also has been proposed.[26] Thus, formation of a π^2-arene complex has been envisioned by Jones and Feher[27] to precede the creation of a σ-complex along the reaction path to C–H bond activation in the $[(\eta^5\text{-Cp}^*)Rh(PMe_3)]$ intermediate (Cp* = pentamethylcyclopentadienyl). On the other hand, Stoutland and Bergman have demonstrated conclusively that attack at a C–H bond in ethylene precedes π-complex formation by ethylene and $[(\eta^5\text{-Cp}^*)Ir(PMe_3)]$, which affords $(\eta^5\text{-Cp}^*)Ir(PMe_3)(CH_2{=}CH_2)$.[28] To

(17) Dennenberg, R. J.; Darensbourg, D. J. *Inorg. Chem.* **1972**, *11*, 72.
(18) van Eldik, R.; Asano, T.; Le Noble, W. J., *Chem. Rev.* **1989**, *89*, 549 and references cited therein.
(19) Experiments at low [pip] could not be carried out at ambient temperature at pressures >80 MPa because benzene freezes under these conditions.
(20) The compressibility of benzene, 0.994 GPa^{-1}, is less than that observed for *n*-heptane, 1.3 GPa^{-1}; yet no curvature of plots of ln k vs P after flash photolysis of $Cr(CO)_6$ in the presence of L is noted in the latter solvent: Dobson, G. R.; van Eldik, R.; Zhang, S.; Bajaj, H. C.; Zang, V. Unpublished results.
(21) Stolz, I. W.; Haas, H.; Sheline, R. K. *J. Am. Chem. Soc.* **1965**, *87*, 715.
(22) Harman, W. D.; Sekine, M.; Taube, H. *J. Am. Chem. Soc.* **1988**, *110*, 5725.
(23) (a) Browning, J.; Green, M.; Penfold, B. R.; Spencer, J. L.; Stone, F. G. A. *J. Chem. Soc., Chem. Commun.* **1973**, 31. (b) Browning, J.; Penfold, J. R. *J. Cryst. Mol. Struct.* **1974**, *4*, 335. (c) Cobbledick, R. E.; Einstein, F. W. B. *Acta Crystallogr.* **1978**, *B34*, 1849. (d) Sweet, J. R.; Graham, W. A. G. *J. Am. Chem. Soc.* **1983**, *105*, 305. (e) van der Heijden, H.; Orpen, A. G.; Pasman, P. *J. Chem. Soc., Chem. Commun.* **1985**, 1576. (f) Belt, S. T.; Duckett, S. B.; Perutz, R. N. *J. Chem. Soc., Chem. Commun.* **1989**, 928. (g) Jones, W. D.; Dong, L. *J. Am. Chem. Soc.* **1989**, *111*, 8722.
(24) Brookhart, M.; Green, M. L. H. *J. Organomet. Chem.* **1983**, *250*, 395.
(25) Saillard, J. Y.; Hoffmann, R. *J. Am. Chem. Soc.* **1984**, *106*, 2006.
(26) Crabtree, R. H.; Hamilton, D. G. *Adv. Organomet. Chem.* **1988**, *28*, 299.
(27) Jones, W. D.; Feher, F. *J. Am. Chem. Soc.* **1984**, *106*, 1650.

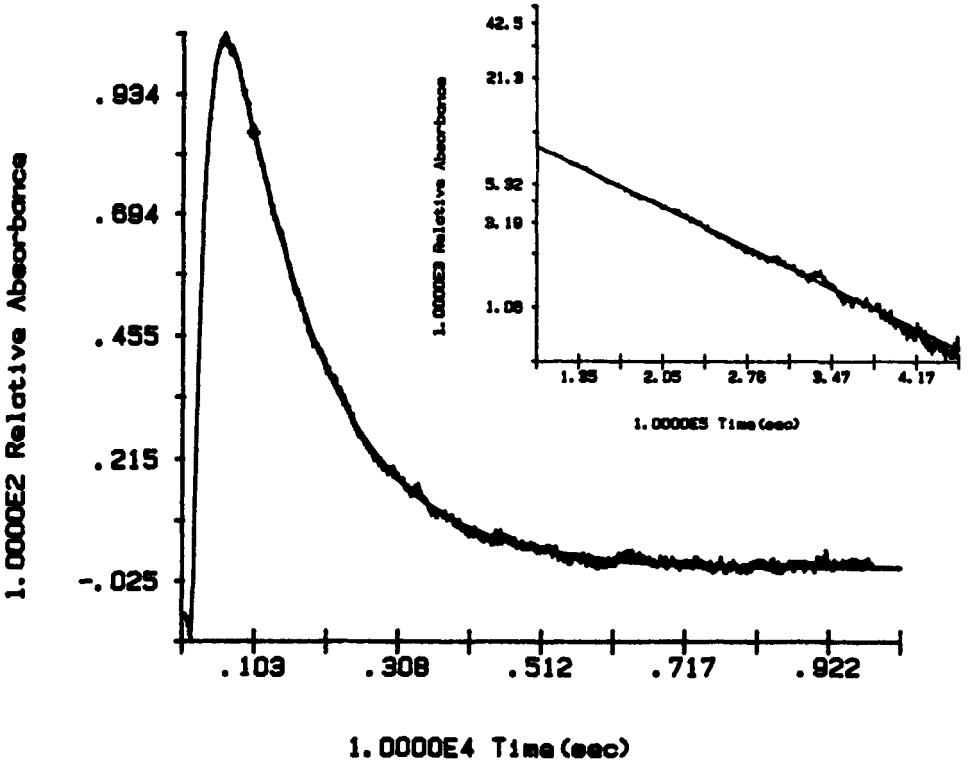

Figure 3. Plot of absorbance vs time monitored at 490 nm for the reaction taking place after flash photolysis of $Cr(CO)_6$ in piperidine (2.085 M)/benzene (8.996 M) solution at 25.0 °C. The inset shows the data plotted as ln $(A_t - A_\infty)$ vs time.

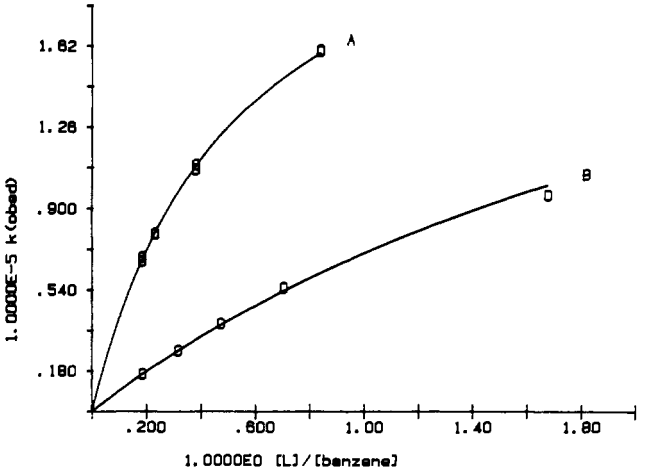

Figure 4. Plots of k_{obsd} vs [L]/[benzene] (L = piperidine (A), 1-hexene (B)) for reactions taking place after flash photolysis of $Cr(CO)_6$ in L/benzene solutions at 25.0 °C.

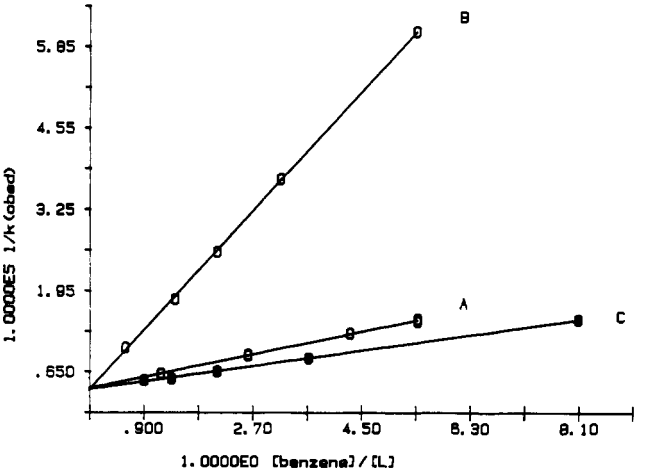

Figure 5. Plots of $1/k_{obsd}$ vs [benzene]/[L] (L = piperidine (A), 1-hexene (B)) and $1/(k_{obsd} - k_3[py])$ vs [benzene]/[py] (py = pyridine (C)) for reactions taking place after flash photolysis of $Cr(CO)_6$ in L/benzene solutions at 25.0 °C.

probe the bonding possibilities in **1**, flash photolysis of $Cr(CO)_6$/bz-d_6/pip solutions also was investigated. Figure 7 compares plots of $1/k_{obsd}$ vs [bz]/[pip] and $1/k_{obsd}$ vs [bz-d_6]/[pip] at 25.0 °C (eq 4), which afford the ratios $k_{1H}/k_{1D} = 0.81$ (5) and $k_{-1H}/k_{-1D} = 0.67$ (6). These ratios are indicative of weak "inverse" kinetic isotope effects for benzene–Cr bond breaking and bond formation. Thus the present results support more H–Cr bonding in the transition state(s) leading to formation of **1** and **2** (eq 2) than in **1** and **2** themselves. This in turn would suggest that bonding in **1** involves an isolated double bond while in the transition state agostic C–H–Cr bonding or formation of a σ-complex may be taking place. Note that the negative value observed for $\Delta V_2^* - \Delta V_{-1}^*$ (vide supra), suggestive of less volume collapse for addition of bz vs pip to $[Cr(CO)_5]$, may also indicate "side-on" bonding of bz to Cr. A comparison of the rates of *n*-octane (oct) displacement by hex from photogenerated $[(oct)Cr(CO)_5]$ and $[(oct\text{-}d_{18})Cr(CO)_5]$ transients has afforded a "normal" deuterium kinetic isotope effect ($k_H/k_D = 1.4$ (2)),[29] as would be anticipated for oct C–H–Cr bond *breaking* in the transition state.

While Parkin and Bercaw recently have indicated that there is no definitive experimental evidence that a single elementary step exhibits an inverse primary kinetic isotope effect and that all inverse primary kinetic isotope effects may be explained by the occurrence of a preequilibrium,[30] it has been noted, both empirically[31] and theoretically,[32] that the kinetic deuterium isotope effect may become inverse for an elementary reaction. A hypo-

(28) (a) Stoutland, P. O.; Bergman, R. G. *J. Am. Chem. Soc.* **1985**, *107*, 4581. (b) Stoutland, P. O.; Bergman, R. G. *J. Am. Chem. Soc.* **1988**, *110*, 5732.

(29) Dobson, G. R.; Zhang, S. Unpublished results.
(30) Parkin, G.; Bercaw, J. E. *Organometallics* **1989**, *8*, 1172.
(31) (a) Creemers, H. M. J. C.; Verbeek, F.; Noltes, J. G. *J. Organomet. Chem.* **1967**, *8*, 469. (b) Leusink, A. J.; Budding, H. A.; Drenth, W. *J. Organomet. Chem.* **1967**, *9*, 295.
(32) (a) Bigeleisen, J. *Pure Appl. Chem.* **1964**, *8*, 217. (b) Melander, L. *Acta Chem. Scand.* **1971**, *25*, 3821.

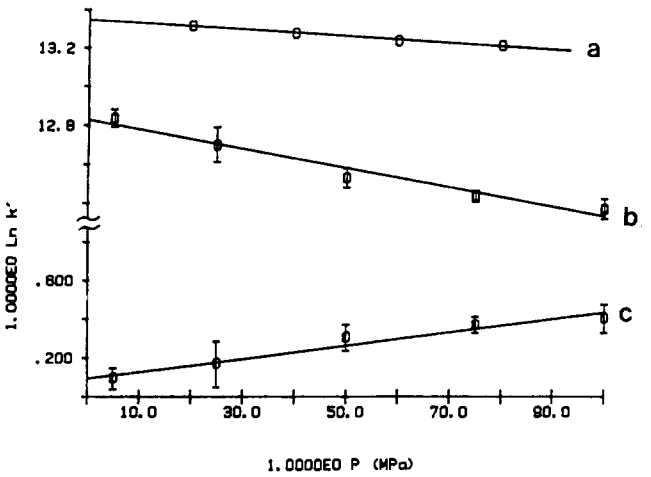

Figure 6. Plots of (a) ln (k_1k_2/k_{-1}) vs P, (b) ln k_1 vs P, and (c) ln (k_2/k_{-1}) vs P for reactions at various pressures after flash photolysis of $Cr(CO)_6$/benzene/piperidine solutions at 25.0 °C.

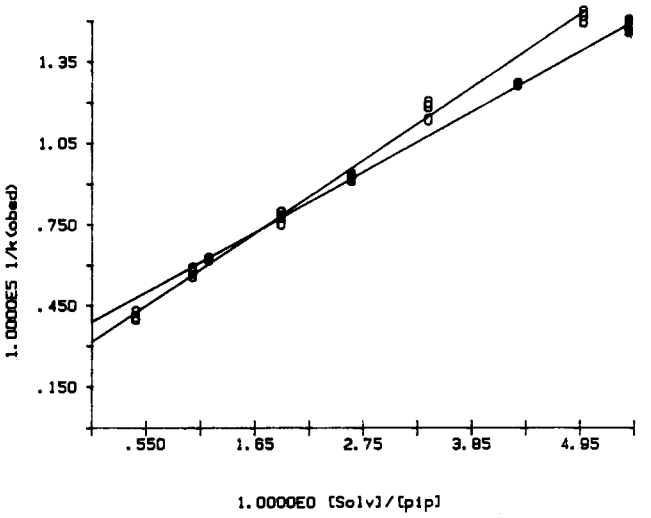

Figure 7. Plots of (○) $1/k_{obsd}$ vs [benzene]/[piperidine] and (●) $1/k_{obsd}$ vs [benzene-d_6]/[piperidine] for reactions after flash photolysis of $Cr(CO)_6$/benzene/piperidine and $Cr(CO)_6$/benzene-d_6/piperidine solutions, respectively.

thetical potential energy vs reaction coordinate diagram that illustrates the observed results in terms of the two ground states and a common transition state is shown in Figure 8. While the difference in zero-point energies in the transition state (Δ_2) may arise from both Cr–H(D) and C–H(D) interactions, the difference in zero-point energies for the ground states (Δ_1, Δ_3) are envisioned to arise from C–H(D) interactions in η^2-coordinated and free benzene molecules. To account for the observed kinetic isotope effects, $\Delta_2 > \Delta_1 > \Delta_3$, since $k_{1H}/k_{1D} < 1$, $k_{-1H}/k_{-1D} < 1$, and $k_H/k_D = (k_{1H}/k_{1D})/(k_{-1H}/k_{-1D})$ (or $(k_{1H}/k_{-1H})/(k_{1D}/k_{-1D})$) = 1.2 (2) > 1. The slight difference between Δ_1 and Δ_2 may be

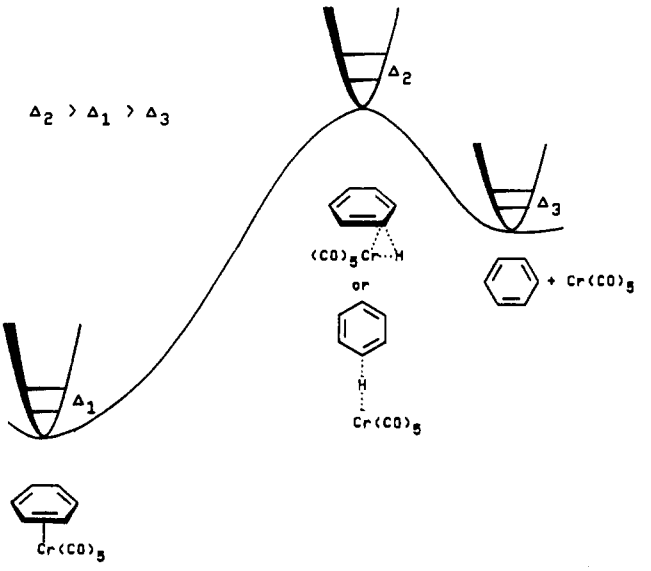

Figure 8. Plot of potential energy vs the reaction coordinate for solvation/desolvation of $[(\eta^2\text{-benzene})Cr(CO)_5]$.

attributable to secondary isotope effects.[33] Streitwieser et al. have proposed that such an isotope effect might arise from the change in frequency of out-of-plane C–H bending modes for sp^2- and sp^3-hydridized carbons.[34] Applying the Streitwieser concept to the interaction of Cr to an isolated double bond of benzene, which is accompanied by the sp^2 to sp^3 rehybridization of the two carbon atoms involved, one would expect a greater zero-point energy difference in η^2-coordinated benzene than in free benzene, as is observed. However, since the interaction of benzene with $[Cr(CO)_5]$ is relatively weak overall, secondary isotope effects might not be expected to be important in the transition state.

Acknowledgment. The support of this research by the National Science Foundation under Grant CHE-8800127 (G.R.D) and the Deutsche Forschungsgemeinschaft and the Volkswagen-Stiftung (R.v.E.) is gratefully acknowledged. The high-pressure experiments and analyses of the data produced were performed at the Center for Fast Kinetics Research (CFKR), University of Texas at Austin. The CFKR is supported jointly by the Biomedical Research Technology Program of the Division of Research Resources of NIH (Grant RR000886) and by the University of Texas at Austin. The advice and technical assistance of the staff at CFKR are much appreciated.

Supplementary Material Available: Appendix A, giving a listing of rate constants for reactions taking place after flash photolysis of $Cr(CO)_6$ in benzene/L and benzene-d_6/L solutions (L = piperidine, 1-hexene, pyridine) at various temperatures and pressures (8 pages). Ordering information is given on any current masthead page.

(33) Strausz, O. P.; Safarik, I.; O'Callaghan, W. B.; Gunning, H. E. *J. Am. Chem. Soc.* **1972**, *94*, 1828.
(34) Streitwieser, A., Jr.; Jagow, R. H.; Fahey, R. C.; Suzuki, S. *J. Am. Chem. Soc.* **1958**, *80*, 2326.